Optimal Placement of Tuning Masses for Vibration Reduction in Helicopter Rotor Blades

Jocelyn I. Pritchard* and Howard M. Adelman†
NASA Langley Research Center, Hampton, Virginia

This paper describes methods for reducing vibration in helicopter rotor blades by determining the optimum sizes and locations of tuning masses through formal mathematical optimization techniques. An optimization procedure is developed that employs the tuning masses and corresponding locations as design variables that are systematically changed to achieve low values of shear without a large mass penalty. The finite-element dynamic analysis of the blade and the optimization formulation require the development of discretized expressions for two performance parameters: the modal shaping parameter and the modal shear amplitude. Matrix expressions for both quantities are derived in this paper. Three optimization strategies are developed and tested. The first is based on minimizing the modal shaping parameter, which indirectly reduces the modal shear amplitudes corresponding to each harmonic of airload. The second strategy reduces these amplitudes directly, and the third strategy reduces the shear as a function of time during a revolution of the blade. The first strategy works well for reducing the shear for one mode responding to a single harmonic of the airload but has been found in some cases to be ineffective for more than one mode. The second and third strategies give similar results and show excellent reduction of the shear with a low mass penalty.

Nomenclature

A_k = amplitude of the generalized force distribution
DAF_{ik} = dynamic amplification factor
F_{ik} = generalized force, lbf
$\{F_k\}$ = force vector, lbf
f, f_0 = objective function
g, g_0 = constraint function
$\mathscr{I}$ = set of modes included in procedure
$\mathscr{K}$ = set of harmonics of airload included in procedure
$[K]$ = elastic stiffness matrix, lbf/in.
$[M]$ = mass matrix, lbm
$\bar{M}_i$ = generalized mass, lbm
M_n = tuning mass, lbm
MSP = modal shaping parameter
M_{TOT} = total tuning mass, lbm
m = mass per unit length, lbm/in.
$NCON$ = number of constraints
NDV = number of design variables
$NHARM$ = number of harmonics of airload included in procedure
$NMASS$ = number of tuning masses included in procedure
$NMODE$ = number of modes included in procedure
$NTIME$ = number of critical time points in one revolution of blade
q_{ik} = response of ith mode subject to k/rev harmonic of airload
$|q_{ik}|$ = amplitude of the response of ith mode to k/rev harmonic of airload
S = amplitude of the blade root vertical shear force, lbf
S_{ik} = amplitude of the modal shear force corresponding to the ith mode and k/rev harmonic of airload, lbf
S_k = amplitude of the shear force associated with the k/rev harmonic of airload, lbf
s = time variation of blade root vertical shear force, lbf
s_{ik} = time variation of modal shear force corresponding to ith mode and k/rev harmonic of airload, lbf
t = time, s
t_m = critical time, s
v_j = jth design variable
$s_{\max}$ = maximum peak shear in one blade revolution, lbf
X_n = locations of the tuning masses along blade span, in.
$\beta, \beta_k, \beta_{ik}$ = additional design variables
ζ_i = damping coefficient
ϕ_k = phase angle of k/rev harmonic
$\{\phi_i\}$ = eigenvector for ith mode
γ_{ik} = phase angle
ω_i^2 = eigenvalue equal to the square of the ith natural frequency, rad/s^2
Ω = angular velocity of blade, rpm or rad/s
ω_{li} = lower bound on frequency, rad/s
ω_{ui} = upper bound on frequency, rad/s
Δv_j = change in jth design variable

Subscripts and Superscripts

i = ith mode
j = jth design variable
k = kth harmonic of airload
T = transpose of a matrix

Introduction

THE current trend in engineering design of aircraft and spacecraft is to incorporate critical requirements from all pertinent disciplines analytically in an early phase of the design process to avoid the costly modification of a prototype

Presented as Paper 88-2312 at the AIAA/ASME/ASCE 29th Structures, Structural Dynamics, and Materials Conference, Williamsburg, VA, April 18-20, 1988; received May 5, 1988; revision received Feb. 25, 1989.

*Research Engineer.
†Deputy Head Interdisciplinary Research Office.

after a problem has been detected.[1] Incorporation of vibration requirements in rotorcraft design is one example of this. In helicopter rotor blade and fuselage design, the need to increase ride comfort, stability, and fatigue life of structural components leads to stringent design constraints on vibration levels.[2-4]

Vibration is transmitted from the blade to the fuselage primarily through a time-dependent shear force at the hub. Historically, frequency placement has been the principal technique for reducing rotor blade vibration.[5,6] Recently it has been shown that minimization of the hub shear can be achieved through minimization of a modal shaping parameter (*MSP*).[2,3] An associated technique, sometimes referred to as "modal shaping" or "modal tailoring," alters the vibration mode shapes of the blades through mass and/or stiffness modification to make them less responsive to the airloads.[2,7-9] A number of passive control techniques show promise for overall reduction of structural vibration in rotor blades. For example, pendulum absorbers,[10] active isolation devices,[11] additional damping,[4,11,12] and vibration absorbers that create antiresonances[13,14] have been demonstrated. Particularly effective is the strategic placement of tuning masses along the blade span to tailor mode shapes.[2,3,5] What has been lacking in modal shaping and frequency placement methods is a systematic approach for predicting the best locations for the tuning masses along the blade span.

The purpose of this paper is to develop and demonstrate a method for optimally locating, as well as sizing, tuning masses to reduce vibration using formal mathematical optimization techniques. The design goal is to find the best combination of tuning masses and their locations to minimize blade root vertical shear without a large mass penalty. The method is to formulate and solve an optimization problem in which the tuning masses and their locations are design variables that minimize a combination of blade shear and the added mass with constraints on frequencies to avoid resonance.

The optimization procedure includes a finite-element vibration analysis[15] of a rotor blade in combination with a general-purpose optimization code.[16] An explicit, approximate analysis[17] of the blade vibration behavior is used to avoid the high computational cost of repeating the finite-element analysis for every blade modification. An analytical sensitivity capability is incorporated into the optimization procedure.

Three alternate optimization strategies are developed and demonstrated in the paper. The first is based on minimizing the modal shaping parameter, thus reducing amplitudes of the modal shear for a single mode and single harmonic of the airloading. The second strategy directly reduces the shear amplitudes corresponding to several harmonics for several modes, and the third strategy reduces the total shear as a function of time during a revolution of the blade. Results are shown in which the described strategies are applied to a rotor blade design considering single-mode/single-harmonic airload as well as multiple-mode/multiple-harmonic airload cases.

Rotor Blade Dynamic Analysis Considerations

Calculation of the natural vibration mode shapes and frequencies and the steady-state harmonic response are the fundamental analysis steps in the optimization procedure to be described. The purpose of this section of the paper is to outline the analytical basis and modeling conventions for the calculations.

The rotor blade is modeled as a pinned-free beam undergoing lateral vibration normal to the plane of the rotor disk. This "flapwise" motion is in general accompanied by in-plane (edgewise) motion as well as torsion, but these are not included in this work. The beam is assumed to rotate at a constant speed (the rotor speed) about an axis that passes through the pinned end of the beam and is normal to the rotor disk. The effects of blade rotation are included through the centrifugal and differential stiffness terms in the equation of motion. An additional term due to the Coriolis acceleration generally occurring in the equations of motion of rotating structures is not necessary in the model used herein. Also, damping is neglected in the calculation of frequencies and mode shapes, and although it is often included in response calculations as modal damping, damping is neglected in all calculations herein.

The time-dependent forces acting on the rotor blade are associated with the lift and drag forces generated by the airflow passing through the rotor disk. These loads are spatially distributed along the blade and vary with time sinusoidally at frequencies that are integer multiples (harmonics) of the rotor speed. It is customary in rotorcraft dynamics to use the notation N/rev or N per rev when referring to frequencies or loading at N times the rotor speed. In rotor blade dynamic response, it is generally assumed that the loads are specified in terms of distributions and phases for all appropriate harmonics. For an N-bladed rotor, the most critical frequencies of load and response are $N\Omega$ and $(N \pm 1)\Omega$. Thus, the most important harmonics are N and $N \pm 1$.

Derivation of Performance Parameters

The degree to which the design is optimized is measured by two performance parameters: the modal shaping parameter (*MSP*) and the amplitude of the blade root vertical shear S. This section of the paper contains derivations of these performance parameters. The roles they play in the optimization will be discussed in a subsequent section of the paper.

Derivation of MSP and Shear

Reference 2 derives an expression for the vertical shear contribution s_{ik} from the ith flapwise mode due to the kth harmonic of the airload for a distributed parameter model of a rotor blade. This paper develops its finite-element counterpart.

As given by Eq. (11) of Ref. 2, the expression for s_{ik} is

$$s_{ik} = q_{ik} \cdot \omega_i^2 \int m\phi_i \, dx \tag{1}$$

where q_{ik} is the steady-state modal response, ω_i is the ith natural frequency, ϕ_i is the ith eigenvector, and m is the mass per unit length. For a discrete (finite-element modeled) structure, the analogous expression is

$$s_{ik} = q_{ik}\omega_i^2 \{U\}^T [M]\{\phi_i\} \tag{2}$$

where $[M]$ is the diagonal mass matrix and $\{U\}$ is a selection vector that extracts the appropriate components from the eigenvector. For example, for modal shaping of the flapwise modes, $\{U\}$ contains 1.0 in the rows corresponding to the flap degree of freedom and 0.0 elsewhere. The expression for q_{ik} is

$$q_{ik} = |q_{ik}| \sin(k\Omega t + \gamma_{ik}) \tag{3}$$

where

$$|q_{ik}| = \frac{F_{ik}}{\bar{M}_i (k\Omega)^2 \left\{ \left[\left(\frac{\omega_i}{k\Omega} \right)^2 - 1 \right]^2 + \left(\frac{2\xi_i \omega_i}{k\Omega} \right)^2 \right\}^{1/2}} \tag{4}$$

and

$$F_{ik} = A_k \{F_k\}^T \{\phi_i\} \tag{5}$$

A_k is the amplitude of the force, and $\{F_k\}$ is the force distribution for the kth harmonic.

Equation (2) becomes

$$s_{ik} = S_{ik} \sin(k\Omega t + \gamma_{ik}) \tag{6}$$

and

$$s(t) = \sum_k \sum_i S_{ik} \sin(k\Omega t + \gamma_{ik}) \tag{7}$$

where

$$S_{ik} = \frac{\{U\}^T[M]\{\phi_i\}}{\bar{M}_i} \cdot DAF_{ik} \cdot F_{ik} \tag{8}$$

For the case of no damping ($\xi = 0$), the dynamic amplification factor DAF_{ik} is

$$DAF_{ik} = \frac{(\omega_i/k\Omega)^2}{[(\omega_i/k\Omega)^2 - 1]} \tag{9}$$

Using Eqs. (5), (8), and (9) and rearranging terms leads to the expression

$$S_{ik} = \frac{\{U\}^T[M]\{\phi_i\} \cdot \{F_k\}^T\{\phi_i\}}{\bar{M}_i} \cdot DAF_{ik} \cdot A_k \tag{10}$$

The total contribution from all the modes to the kth harmonic of shear is

$$S_k = \sum_i S_{ik} \tag{11}$$

Following Taylor,[2] the first term of Eq. (10) is identified as the modal shaping parameter (*MSP*). Thus,

$$MSP_{ik} = \frac{\{U\}^T[M](\phi_i\} \cdot \{F_k\}^T\{\phi_i\}}{\bar{M}_i} \tag{12}$$

Equation (12) shows that an *MSP* exists for each mode shape and load case (harmonic). Physically, MSP_{ik} is a measure of the shear response corresponding to the ith mode and the kth harmonic of the loading. Since the *MSP* is a function of the mode shape, it is possible to reduce its value by tailoring the mode shape. For example, if the mode shape is made orthogonal to the force distribution, then the value of the *MSP* is zero. As seen from Eq. (10), S_{ik} can be reduced by reducing MSP_{ik} while limiting the size of DAF_{ik}. The size of DAF_{ik} is controlled by placing constraints on the natural frequencies as suggested in Ref. 5. Equations (7), (10), (11), and (12) are the basis for the optimization strategies that will be discussed in the next section of the paper.

Optimization Formulation

Design Goal

The design goal is to find the optimum combination of tuning masses M_n and their locations X_n (Fig. 1) to minimize blade root vertical shear while avoiding an excessive mass penalty. The method is to formulate and solve an optimization problem in which the tuning masses and locations are design variables that minimize the objective function, which is a combination of a measure of vertical shear and the added mass. Additionally, constraints are placed on the frequencies to avoid resonance.

Three optimization strategies will be described in this section of the paper. In each method, additional design variables (β) are used. They facilitate the tradeoff between desired performance and excessive mass penalty. A general-purpose constrained optimization program, CONMIN,[16] is used. CONMIN requires derivatives of the objective function and constraints. All derivatives are obtained analytically.

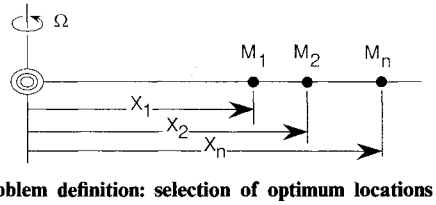

Fig. 1 Problem definition: selection of optimum locations for tuning masses.

Strategy I

The objective function is

$$f = \left(1 + \sum_k \sum_i \beta_{ik}\right) \sum_{n=1}^{NMASS} M_n \tag{13}$$

where i is an element of the set of included modes $\mathscr{I}$ and $\mathscr{K}$ is an element of the set of included harmonics of airload $\mathscr{K}$, M_n are the tuning masses, and β_{ik} are the additional design variables that also appear in the following constraints;

$$g = MSP_{ik} - \beta_{ik} \leq 0 \qquad \begin{matrix} i \epsilon \mathscr{I} \\ k \epsilon \mathscr{K} \end{matrix} \tag{14}$$

These constraints express the requirement that the MSP_{ik} be less than β_{ik}. The convention is that for $g \leq 0$, the constraint is satisfied and violated otherwise. Large values of β_{ik} make the constraints easy to satisfy, but cause a large objective function. Conversely, small values of β_{ik} result in a small objective function, but make the constraints more difficult to satisfy. The optimizer, therefore, will tend toward designs with the lowest posible values of β_{ik} and, therefore, low values of MSP_{ik}. Additional constraints include upper and lower bounds on the frequencies to avoid resonance;

$$\omega_{li}^2 \leq \omega_i^2 \leq \omega_{ui}^2 \tag{15}$$

The required derivatives of the objective function and constraints are obtained by differentiating Eqs. (13–15).

Strategy II

In this strategy the constraints are placed on the harmonic amplitudes S_k[see Eq. (11)]. The objective function is

$$f = \left(1 + \sum_k \beta_k\right) \sum_{n=1}^{NMASS} M_n \tag{16}$$

The additional design variables β_k play a role similar to β_{ik} in the first strategy. Here the constraints are written as

$$g = S_k - \beta_k \leq 0, \qquad k \in \mathscr{K} \tag{17}$$

This strategy also employs upper and lower bound constraints on the frequencies [Eq. (15)]. Similar to strategy I, the derivative of the objective function is obtained by differentiating Eq. (16), and differentiating Eqs. (17) and (15) give the derivatives of the constraints.

Strategy III

In this formulation, the shear as a function of time is minimized by constraining all the peak values that occur during a revolution of the blade. These are called critical point constraints,[18] The objective function is

$$f = [1 + \beta] \sum_{n=1}^{NMASS} M_n \tag{18}$$

and the constraints are

$$g = s(t_m) - \beta \leq 0, \qquad m = 1, 2, \ldots, NTIME \tag{19}$$

which require that the values of the shear at each time t_m be less than the value of β, and again β is minimized because of its role in the objective function. As shown in Eq. (7), $s(t_m)$ is the shear at time t_m where t_m represents a time at which a peak occurs in $s(t)$.

The peak values are identified as follows. A value of *NTIME* is specified corresponding to the maximum number of peaks in the function $s(t)$ during a revolution of the blade. The peak values are identified by examining the shear as a function of time.[18] The constraints are placed on these *NTIME* values of shear to force the peaks to be as small as

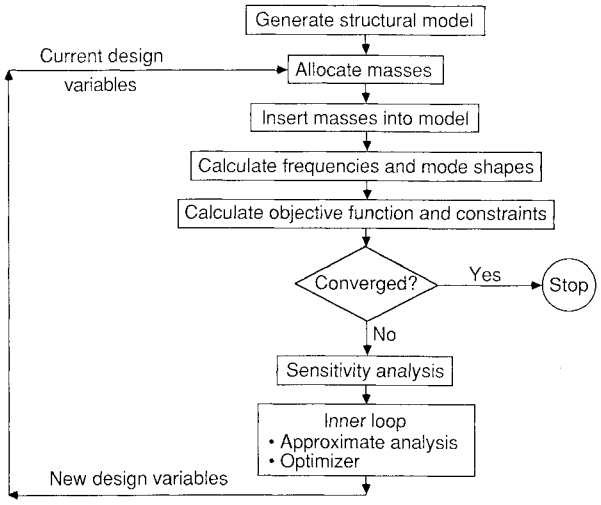

Fig. 2 Flow chart for optimization procedure.

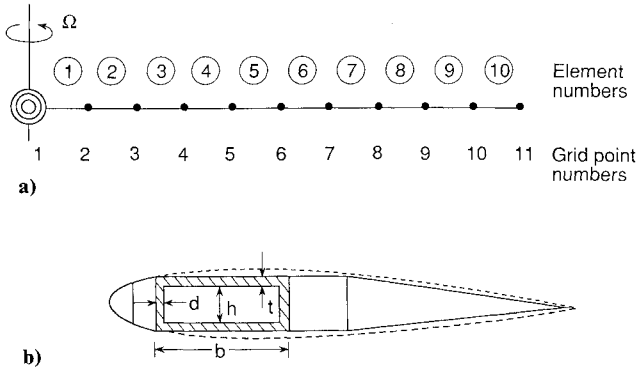

Fig. 3 Test problem: a) finite-element model of rotor blade (10 equal elements); b) cross-sectional detail of rotor blade.

Table 1 Details of finite-element model of rotor blade

Material properties and cross-sectional dimensions (see Fig. 4)						
Element	E psi	ρ, lb/in.^{3}	b, in.	h, in.	t, in.	d, in.
1	0.490×10^7	0.07	3.75	2.50	0.80	0.10
2–10	0.585×10^7	0.07	3.75	2.50	0.80	0.10

Initial values of design variables (see Fig. 1)					
X_1, in.	X_2, in.	X_3, in.	M_1, lbm	M_2, lbm	M_3, lbm
135.10	154.40	173.70	5.21	6.55	6.60

Blade characteristics			
Length, in.	Structural mass, lbm	Nonstructural mass, lbm	Ω rpm
193	87.82	122.93	425

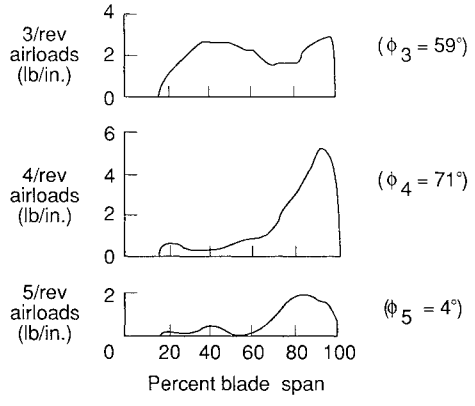

Fig. 4 Amplitude distributions and phase angles of airloads.

possible. This procedure does not require that the locations of the peaks be constant throughout the optimization process, since the search for the peaks occurs each time the analysis is performed for a new set of design variables. Additional constraints are again placed on the upper and lower values of the frequencies [Eq. (15)]. Derivatives of the objective function and constraints are obtained by differentiating Eqs. (18), (19), and (15).

Optimization Procedure

The sequence of operations in the optimization procedure is illustrated in Fig. 2. The overall procedure consists of two nested loops. Each pass through the outer loop is referred to as a cycle that involves a full analysis and a sensitivity calculation. The first step is to generate the finite-element structural model of the beam, excluding the values of tuning masses. The design variables (masses and locations) are used to allocate the masses to the appropriate grid points of the model. Specifically, the masses M_n are divided between the two grid points adjacent to each X_n by prorating according to the distance from each. Next, the masses are inserted into the model, the vibration analysis is performed, and the MSP_{ik} and shear amplitudes S_{ik} are calculated for $NMODE$ number of modes responding to $NHARM$ number of harmonics. The sensitivity analysis includes calculating the vibration mode shape derivatives by Nelson's method[19] and then calculating the derivatives of the objective function and constraints as indicated in the previous section of the paper. The inner loop consists of the optimization program CONMIN[16] and an approximate analysis for calculating the objective function and the constraints (see Ref. 17). The approximate equations are

$$f = f_0 + \sum_{j=1}^{NDV} \frac{\partial f}{\partial v_j} \Delta v_j \tag{20}$$

$$g = g_0 + \sum_{j=1}^{NDV} \frac{\partial g}{\partial v_j} \Delta v_j \tag{21}$$

These equations give the change in the objective function from f_0 to f and the change in a constraint from g_0 to g corresponding to a change in design variable Δv_j. To assure that the linear approximations in Eqs. (20) and (21) are valid, the size of Δv_j is limited to 10% of v_j. Use of these approximations saves computational time and effort in the inner loop, where many evaluations of the objective function and constraints are required. Development of these and other techniques and demonstration of their benefits are described in Ref. 20. Once the inner loop iterations have converged, the next cycle of the outer loop begins, using the current design variables as the new values of the lumped masses and their locations. These masses are then inserted into the structural model, and the process continues until convergence of the outer loop is achieved.

Example Problem

The example problem is a beam representation of an articulated rotor blade developed in Ref. 5 and shown in Fig. 3.

The beam is 193 in. long with a hinged end condition and is modeled by 10 finite elements of equal length. The model contains both structural mass and lumped (nonstructural) masses. The beam has a box cross section as shown in Fig. 3b, and the material properties and cross-sectional dimensions are summarized in Table 1. Three lumped masses are to be placed along the length of the beam. The values of the masses and their locations are the design variables, and their initial values, shown in Table 1, are from the blade in Ref. 5.

Figure 4 shows the distributions (from Ref. 2) and phase angles (from Ref. 21) of the airloads used. They are input as tabulated values of distributed forces (i.e., force per unit length) into the finite-element analysis (Ref. 15). The forces $\{F_k\}^T$ needed in Eq. (5) are calculated as consistent nodal forces for the finite-element model. These airloads represent the 3-, 4-, and 5-per-rev lifting airloads that are typical of a four-bladed articulated rotor system. These harmonics were chosen because they are the prime contributors to the vibration of a four-bladed rotor system. In this work, the first and second elastic flapping modes are included because they are prime contributors to the vertical vibration transmitted by the rotor blades to the fuselage.

Results and Discussion

The following sections discuss results obtained for each of the three optimization strategies applied to the example problem. The test cases include 1) a single mode responding to a single harmonic of the airload, 2) two modes responding to a single harmonic of the airload, and 3) two modes responding to three harmonics of the airload.

Results for Strategy I

Figures 5a and 5b show the initial and final designs for the first test case using strategy I for minimizing S_{14}, the shear for the first elastic flapping mode, and the 4/rev airload by proper placement of three tuning masses. The 4/rev airload is concentrated at the tip of the blade, and in order to shape the mode to be insensitive to the airload, all three tuning masses were moved to the tip of the blade. Figure 5c shows a sketch of the mode shape before and after optimization. It is this change in the mode shape that reduces the value of the MSP_{14} 99% and the corresponding shear S_{14} by a similar amount. Table 2 summarizes the initial and final designs. It is noted that the large change in MSP and shear is accompanied by an almost zero change in frequency.

This method proved to be very useful when working on the response of one mode corresponding to one airload. However, when this method was applied to more than one mode, it was not always effective. The method did reduce the values of the MSP as required, but low values of the MSP did not necessarily give low values for the shear S_k. The reason for this is that the various MSP (and, therefore, the corresponding contributions to the shear S_{ik}) may have different signs. When these shear contributions are added together [see Eq. (11)], small values for the individual contributions S_{ik} do not always minimize the shear S_k unless the necessary cancelling of equal and opposite terms occurs.

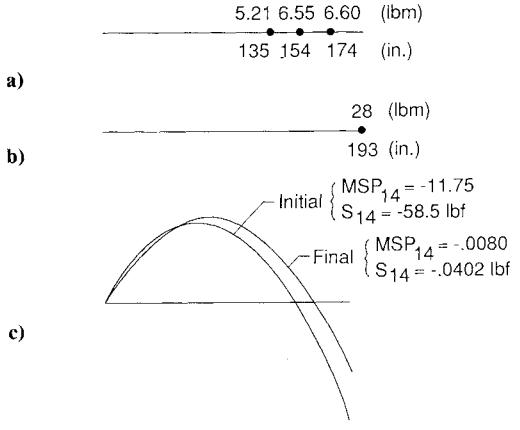

Fig. 5 Initial and final designs for one-mode/one-load case using strategy I: a) initial masses and locations; b) final masses and locations; c) initial and final mode shapes.

Results for Strategy II

In strategy II, the method is to reduce the values of the shear contributions S_{ik} summed over the modes [see Eq. (11)]. This eliminates the problem in strategy I, since constraints placed on the sums of the modal shears encourage the desirable cancellation effects. The first step in demonstrating this method was to validate it for the one-mode/one-load case. The design for strategy II is essentially identical to that of Fig. 5, and Table 2 gives the initial and final designs of the blade. The next step was to apply this strategy to a two-mode/one-load case. The response of the first and second elastic flapping modes corresponding to the 4/rev airload is minimized. Table 3 summarizes the initial and final designs. The initial shear S_4, including both modes, is -34.68 lbf, which is reduced by the optimization process to -0.01 lbf with an accompanying decrease in the added mass.

Inspection of the initial and final values of the MSP (Table 3) shows that the magnitudes of the MSP became larger. This helps to explain the lack of success of strategy I for this problem. In fact, the modal shears S_{14} and S_{24} are equal and opposite, thus combining together to produce a near-zero value of total shear. Figures 6a and 6b show the initial and final masses and their locations, and Fig. 6c shows the change in the shapes of the first and second elastic flapwise modes.

Table 2 Initial and final designs using strategies I and II for one-mode/one-load problem (first elastic flapwise mode at 4/rev

	Initial	Final	
		Strategy I	Strategy II
X_1 in.	135.10	193.00	193.00
X_2, in.	154.40	193.00	193.00
X_3, in.	173.70	193.00	193.00
M_1, lbm	5.21	6.30	6.70
M_2, lbm	6.55	10.53	10.33
M_3, lbm	6.60	10.60	10.40
M_{TOT}, lbm	18.36	27.43	27.43
MSP_{14}	−11.75	−0.008	−0.010
S_{14}, lbf	−58.50	−0.040	−0.051
ω_1, per rev	2.69	2.70	2.70

Table 3 Initial and final designs using strategy II for two-mode/one-load problem (first and second elastic flapwise modes at 4/rev

	Initial	Final
X_1, in.	135.10	135.02
X_2, in.	154.40	146.38
X_3, in.	173.70	157.72
M_1, lbm	5.21	7.15
M_2, lbm	6.55	5.24
M_3, lbm	6.60	0.97
M_{TOT}, lbm	18.36	13.36
S_4, lbf	−34.68	−0.01
S_{14}, lbf	−58.50	−66.91
S_{24}, lbf	23.82	66.90
MSP_{14}	−11.75	−14.61
MSP_{24}	1.03	2.24
ω_1, per rev	2.69	2.63
ω_2, per rev	4.65	4.47

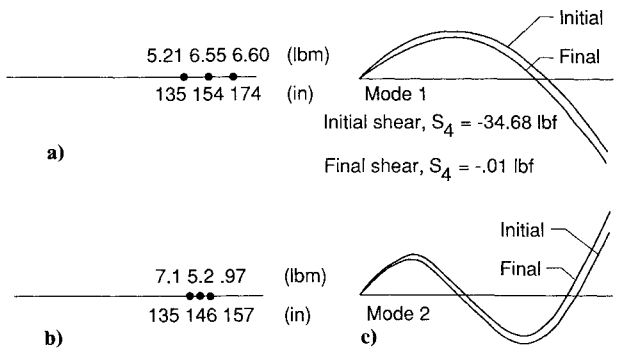

Fig. 6 Initial and final designs for two-mode/one-load case using strategy II: a) initial masses and locations; b) final masses and locations; c) initial and final mode shapes.

Table 4 Initial and final designs using strategies II and III for two-mode/three-load problem (first and second elastic flapwise modes at 3, 4, and 5 per rev

	Initial	Final	
		Strategy II	Strategy III
X_1, in	135.10	150.95	152.81
X_2, in	154.40	154.44	154.27
X_3, in	173.70	154.40	154.42
M_1, lbm	5.21	4.28	7.93
M_2, lbm	6.55	12.40	9.66
M_3, lbm	6.60	10.13	9.26
M_{TOT}, lbm	18.36	26.81	26.85
S_3, lbf	−7.98	−0.36	—
S_4, lbf	−34.68	0.30	—
S_5, lbf	−39.48	−0.16	—
s_{max}, lbf	−78.00	—	−0.58
ω_1, per rev	2.69	2.81	2.81
ω_2, per rev	4.65	4.72	4.72

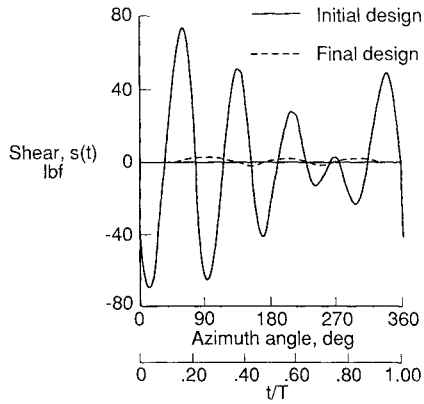

Fig. 7 Time history of blade vertical root shear during one revolution. Initial and final designs for two-mode/three-load case using strategy II.

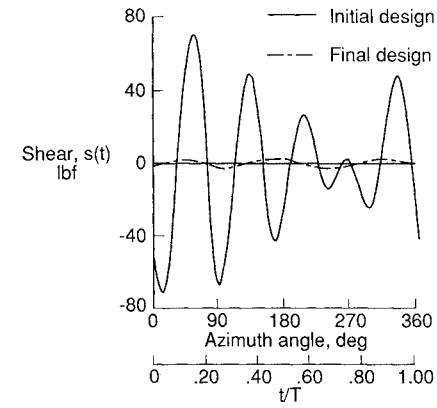

Fig. 8 Time history of blade vertical root shear during one revolution. Initial and final designs for two-mode/three-load case using strategy III.

Table 5 Comparison of peak values of shear during one revolution of the blade using strategies II and III

Strategy II		Strategy III	
$s(t_m)$, lbf	$t_m(s)$	$s(t_m)$, lbf	$t_m(s)$
−0.348	0.009	0.330	0.000
0.198	0.024	−0.186	0.014
0.162	0.044	0.234	0.042
−0.528	0.059	−0.390	0.059
0.756	0.075	0.510	0.075
−0.768	0.092	−0.576	0.090
−0.588	0.107	0.570	0.107
−0.402	0.121	−0.504	0.123
0.354	0.136	0.366	0.138
0.132	0.141	—	—

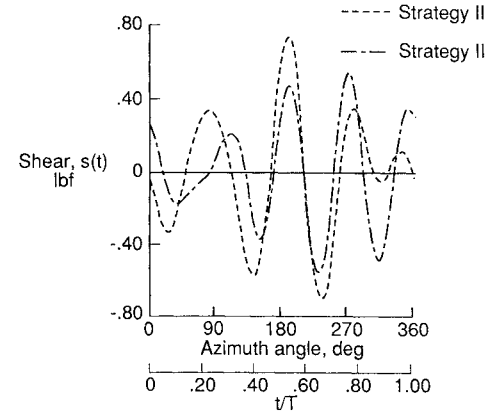

Fig. 9 Comparison of final designs from strategies II and III for two-mode/three-load case.

Strategy II was next applied to a case of two modes responding to the 3-, 4-, and 5-per-rev harmonics of airloading (see Fig. 4). Table 4 shows the initial and final results where the amplitudes of the shears, due to the two flapwise modes, have been reduced significantly with only a 9-lbm increase in tuning mass (note the total blade mass is 211 lbm). For example, S_5, the shear force associated with the 5/rev harmonic, was reduced from −39.48 lbf to −0.162 lbf. Figure 7 gives a time history of the shear during one revolution of the blade before and after optimization. It is clear from the figure that reducing the amplitudes of the harmonic shears results in a large reduction of the total shear throughout a revolution of the blade.

Results for Strategy III

The third strategy was applied to the previous test case of two modes responding to three harmonics. Figure 8 shows graphs of the shear $s(t)$ plotted as a function of time and azimuth for a revolution of the blade for the initial and final designs. The peaks on the initial curve have been reduced dramatically. For example, the maximum peak s_{max} for the initial design is −78.00 lbf, and for the final design the

maximum peak is −0.576 lbf. The extreme right column in Table 4 gives details of the final designs from strategy III and indicates a large payoff for a relatively small increase in added mass.

Comparison of Strategies II and III

As seen from Table 4, strategy III gave a design comparable to strategy II. In both cases, there was a significant reduction in the total shear. Results from strategies II and III are compared in Table 5 in terms of the peak values of $s(t)$ at the critical points. The final results were very close to strategy III, producing slightly lower values for some of the peaks, and strategy II producing lower values of others. Overall, strategy III was slightly better in minimizing the peak shear. Figure 9 shows the shears plotted as functions of time from each strategy. Strategy III was a somewhat more complicated approach than strategy II and was more cumbersome to implement. However, the greater degree of rigor in strategy III makes the slightly greater effort worth the investment.

Concluding Remarks

This paper described methods for systematically locating, as well as sizing, tuning masses to reduce vibration in helicopter rotor blades using formal mathematical optimization techniques. The problem was to find the optimum combination of tuning masses and their locations to reduce vertical shear without a large mass penalty. The methods embodied optimization procedures in which tuning masses and their locations were design variables whose values minimized a combination of shear and added mass. The finite-element dynamic analysis of the blade and the optimization formulations required the development of discretized expressions for two performance parameters: the modal shaping parameter, and the amplitude of the blade root vertical shear. Matrix expressions for both quantities were derived in this paper. The mechanism in the optimization for reducing the vertical blade shear was through "modal shaping" by placing the tuning masses at strategic locations along the blade.

Three optimization strategies were developed. The first was based on minimizing the modal shaping parameter, thus indirectly reducing the amplitudes of the modal shear for each harmonic. The second reduced the shear amplitudes directly, and the third reduced the total shear as a function of time during a revolution of the blade.

Strategy I worked well for reducing the shear for one mode responding to one harmonic of the load, but was ineffective for multiple modes. This was due to the inability of the method to take advantage of sign differences between the contributions for different modes and harmonics. Strategy II worked extremely well for the one-mode/one-load case, as well as multiple mode/multiple loads. Strategy III gave excellent results; i.e. the peak shear was reduced significantly without a large mass penalty. Strategies II and III gave essentially the same results for a two-mode/three-load case. Strategy II is slightly easier to implement, but the fact that strategy III is a more rigorous approach makes it a preferred choice overall.

References

[1]Sobieszczanski-Sobieski, J., "Structural Optimization: Challenges and Opportunities," International Journal of Vehicle Design, Vol. 7, May 1986, pp. 242–263. London, England, June 1983.

[2]Taylor, R. B., "Helicopter Vibration Reduction by Rotor Blade Modal Shaping," 38th Annual Forum of the American Helicopter Society, Paper A-82-38-09-3000, Anaheim, CA, May 1982, pp. 90–101.

[3]Taylor, R. B., "Helicopter Rotor Blade Design for Minimum Vibration," NASA CR-3825, Oct. 1984.

[4]Blackwell, R. H., "Blade Design for Reduced Helicopter Vibration" *Journal of the American Helicopter Society*, Vol. 28, No. 3, July 1983.

[5]Peters, D. A., Ko, T., Korn, A., and Rossow, M. P., "Design of Helicopter Rotor Blades for Desired Placement of Natural Frequencies," 39th Annual Forum of the American Helicopter Society, Paper A-83-39-71-3000, St. Louis, MI, May 1983.

[6]Friedmann, P. P., "Application of Modern Structural Optimization to Vibration Reduction in Rotorcraft," NASA CP-2327, Part 2, Sept. 1984, pp. 553–556.

[7]Davis, M. W., "Optimization of Helicopter Rotor Blade Design for Minimum Vibration," NASA CP-2327, Part 2, Sept. 1984, pp. 609–625.

[8]McCarty, J. L. and Brooks, G. W., "A Dynamic Model Study of the Effect of Added Weight and Other Structural Variations on the Blade Bending Strains of an Experimental Two-Blade Jet-Driven Helicopter in Hovering and Forward Flight," NACA TN-3367, May 1955.

[9]Hirsh, H., Hutton, R. E., and Rasamoff, A., "Effect of Spanwise and Chordwise Mass Distribution on Rotor Blade Cyclic Stresses," *Journal of the American Helicopter Society*, Vol. 1, No. 2, April 1956, pp. 37–45.

[10]Hamouda, M. H. and Pierce, G. A., "Helicopter Vibration Suppression Using Simple Pendulum Absorbers on the Rotor Blade," American Helicopter Society Northeast Region National Specialists' Meeting on Helicopter Vibration, Paper B-81-NE-17-9000, Hartford, CT, Nov. 1981.

[11]Reichert, G., "Helicopter Vibration Control—A Survey," *Vertica*, Vol. 5, No. 1, 1981, pp. 1–20.

[12]Rogers, L., "Damping as a Design Parameter," *Mechanical Engineering*, Vol. 108, No. 1, Jan. 1986.

[13]Wang, B. P., Kitis, L., Pilkey, W. D., and Palazzolo, A., "Synthesis of Dynamic Vibration Absorbers," *Journal of Vibration, Acoustics, Stress, and Reliability in Design*, Vol. 107, April 1985, pp. 161–166.

[14]Kitis, L., Pilkey, W. D., and Wang, B. P., "Optimal Frequency Response Shaping by Appendant Structures," *Journal of Sound and Vibration*, Vol. 95, No. 2, 1984, pp 161–175.

[15]Whetstone, W. D., "Engineering Analysis Language Reference Manual—EISI-EAL System Level, 2091," Engineering Information Systems, Inc., EISI-EAL, July 1983.

[16]Vanderplaats, G. N., "CONMIN—A Fortran Program for Constrained Function Minimization—User's Manual," NASA TM X-62282, Aug. 1973.

[17]Walsh, J. L., "Application of Mathematical Optimization Procedures to a Structural Model of a Large Finite-Element Wing," NASA TM-87597, Jan. 1986.

[18]Haftka, R. T. and Kamat, M. P., *Elements of Structural Optimization*, Martinus Nijhoff Publishers, Dordrecht, The Netherlands, 1985.

[19]Nelson, R. B., "Simplified Calculation of Eigenvector Derivatives," *AIAA Journal*, Vol. 14, Sept. 1976, pp. 1201–1205.

[20]Schmit, L. A. and Farshi, B., "Some Approximation Concepts for Structural Synthesis," *AIAA Journal*, Vol. 12, May, 1974, pp. 692–699.

[21]Hooper, W. E., "The Vibratory Airloading of Helicopter Rotors," *Vertica*, Vol. 8, No. 2, 1984, pp. 73–92.